J|A|C|S
ARTICLES
Published on Web 12/01/2007

A Frequency Domain Existence Proof of Single-Molecule Surface-Enhanced Raman Spectroscopy

Jon A. Dieringer, Robert B. Lettan II, Karl A. Scheidt, and Richard P. Van Duyne*

Northwestern University, Department of Chemistry, 2145 Sheridan Road, Evanston, Illinois 60208

Received September 18, 2007; E-mail: vanduyne@northwestern.edu

Abstract: The existence of single-molecule surface-enhanced Raman spectroscopy (SMSERS) is proven by employing a frequency-domain approach. This is demonstrated using two isotopologues of Rhodamine 6G that offer unique vibrational signatures. When an average of one molecule was adsorbed per silver nanoparticle, only one isotopologue was typically observed under dry N_2 environment. Additionally, the distribution of vibrational frequencies hidden under the ensemble average is revealed by examining the single-molecule spectra. Correlation with transmission electron microscopy reveals that SMSERS active aggregates are composed of multiple randomly sized and shaped nanoparticles. At higher coverage and in a humid environment, adsorbate interchange was detected. Using 2D cross correlation, vibrational modes from different isotopologues were anti-correlated, indicating that the dynamic behavior was from multiple molecules competing for a single hot spot. This allows hot-spot diffusion to be directly observed without analyzing the peak intensity fluctuations.

1. Introduction

In 1997, two independent reports observing single-molecule surface-enhanced Raman spectroscopy (SMSERS) contributed to a reinvigorated interest in surface-enhanced Raman spectroscopy (SERS).[1,2] Nie and Emory reported the observation of SER spectra from single Rhodamine 6G (R6G) molecules adsorbed on citrate-reduced Ag nanoparticles that were electrostatically immobilized on glass in an ambient environment. Strong intensity fluctuations occurred on the seconds time scale and were subsequently attributed to surface diffusion of molecules into and out of the electromagnetic enhancing hot spot.[3,4] Independently, Kneipp et al. observed SMSERS of crystal violet (CV) in citrate-reduced Ag nanoparticle aggregates in solution. Through Brownian sampling, Kneipp observed that the SMSERS signal intensity was quantized and corresponded to 0, 1, 2, and 3 molecules in the probe volume. In addition, the probability of observing *n* molecules followed the Poisson distribution with a fitting parameter of 0.6 molecules, equivalent to the number that was estimated to be in the probe volume. With an order of magnitude increase in the number of molecules adsorbed per nanoparticle, the probabilities were replaced by the Gaussian distribution, and the system approached ensemble-averaged behavior. In both experiments, the authors observed enhancement factors (EF) of $\sim 10^{14}$ in the SERS spectra relative to normal Raman. Although debate concerning the mechanism responsible for these enormous EFs remains, AFM experiments by Brus and co-workers indicate that nanoparticles exhibiting SMSERS are multiparticle aggregates.[5] These results, as well as polarization-modulated SMSERS studies, suggest that the analyte may be located at a junction between two nanoparticles where electromagnetic fields can be significantly enhanced.[6] Here, we will show that the active SMSERS junctions are indeed multinanoparticle aggregates and that the localized suface plasmon resonance (LSPR) results obtained by Brus et al. are confirmed. It should also be noted that, in most SMSERS cases, including this report, the laser excitation is resonant with the electronic absorption of the analyte and therefore this technique should be referred to as single-molecule surface-enhanced resonant Raman spectroscopy (SMSERRS), but for consistency, this report will refer to the phenomenon as simply SMSERS.

To date, most work on SMSERS has focused on fluctuations in the intensity domain, using statistical analysis to support the claim of single-molecule behavior. Rowlen et al. have shown that temporal fluctuation in peak intensity is not adequate evidence of SMSERS.[7] Additionally, Pettinger et al. points out that the SMSERS EF is strongly dependent on the molecule's position in the hot spot and the variations would make the observation of quantized intensity impossible.[8] Doering and Nie provided additional supporting evidence for SMSERS by noting the sudden (minutes time scale) replacement of a R6G SMSERS spectrum by a background spectrum due to citrate adsorption, as well as the sudden appearance of a R6G SMSERS spectrum replacing a citrate backround spectrum.[9] Le Ru and Etchegoin

(1) Nie, S.; Emory, S. R. *Science* **1997**, *275* (5303), 1102−1106.
(2) Kneipp, K.; Wang, Y.; Kneipp, H.; Perelman, L. T.; Itzkan, I.; Dasari, R. R.; Feld, M. S. *Phys. Rev. Lett.* **1997**, *78* (9), 1667−1670.
(3) Bizzarri, A. R.; Cannistraro, S. *Phys. Rev. Lett.* **2005**, *94*, 6.
(4) Weiss, A.; Haran, G. *J. Phys. Chem. B* **2001**, *105* (49), 12348−12354.
(5) Michaels, A. M.; Jiang, J.; Brus, L. *J. Phys. Chem. B* **2000**, *104* (50), 11965−11971.
(6) Bosnick, K. A.; Jiang, J.; Brus, L. E. *J. Phys. Chem. B* **2002**, *106* (33), 8096−8099.
(7) Andersen, P. C.; Jacobson, M. L.; Rowlen, K. L. *J. Phys. Chem. B* **2004**, *108* (7), 2148−2153.
(8) Domke, K. F.; Zhang, D.; Pettinger, B. *J. Phys. Chem. C* **2007**, *111* (24), 8611−8616.

Scheme 1. Chemical Structure of the Two Isotopologues, R6G-d_4 and R6G-d_0

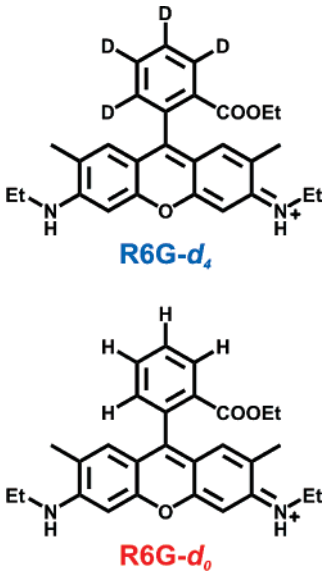

significantly improved the competing adsorbate approach with a systematic study using two different competing analytes (e.g., R6G and benzotriazole).[10−12] It should be noted that the work presented in these references is carried out at surface coverages corresponding to a few hundred molecules per nanoparticle. Furthermore, the interpretation of the results using two different competing adsorbates requires knowledge of the differences in Raman cross section, absorption spectra, and surface binding affinity for the different analytes used. Similar considerations hold for two other reports using the bi-analyte approach.[13,14] Pettinger et al.[8] have reiterated the point that Raman cross-sectional differences and variations in the surface chemistries for the two different adsorbates must be taken into account.

The work reported herein aims to build upon the precedent work on the two-analyte approach cited above, while circumventing its problematic issues. Two isotopologues of Rhodamine 6G, R6G-d_0 and R6G-d_4, are used to demonstrate single-molecule character in the SER spectra. The chemical structures of both isotopologues (chemical species that differ only in the isotopic composition of their atoms) are given in Scheme 1. The use of two isotopologues provides a novel pathway to performing dual analyte single-molecule SERS studies because the electronic absorption spectrum of the adsorbate is not perturbed, the surface chemistry remains unchanged, and the overall Raman cross section is identical. However, the vibrational bands having contributions from C−D stretching and bending will change in intensity and frequency, allowing the two isotopologues to be spectrally resolved. The frequency domain approach using two isotopologues of R6G permits single-molecule behavior to be verified by tracking the spectral signature of the individual species. When sufficiently low concentrations of both analyte molecules are introduced to a solution of silver nanoparticles such that, on average, only one type of molecule is adsorbed to each nanoparticle, each SMSER spectrum contains spectral features of only a single isotopologue. On the other hand, as the coverage is increased such that both analytes should be present on a single nanoparticle, one should observe the vibrational characteristics of both analytes. Thus, one can distinguish single- versus multi-molecule SERS by the number of peaks in the SERS spectrum.

In addition, this work adds considerably to the study of the effect of the nanoparticle environment on single-molecule SERS which has only received brief attention previously. Haran et al. have shown that the nanoparticle environment correlates with the "blinking" character observed in wet systems.[15,16] Also, the blinking phenomenon of SERS has been shown to be oxygen mediated.[17] Here, the system will be kept in a dry N_2 environment for the initial experiments in order to minimize the dynamic behavior. Later, a dynamic system under ambient lab air will be explored and the time evolution will be analyzed.

2. Experimental Section

Rhodamine 6G-d_4 Synthesis. The synthesis of the rhodamine carboxylic acid-d_4 was carried out via the conditions given by Zhang et al.[18] The synthesis of Rhodamine 6G-d_4 (R6G-d_4) was carried out using the general procedure by Almeida et al. [19] (Scheme 1). All reactions were carried out under a nitrogen atmosphere in flame-dried glassware with magnetic stirring. Ethanol (absolute) and *o*-dichlorobenzene (anhydrous, 99%) were used as received from Sigma-Aldrich Chemical Co. To a round-bottom flask equipped with a magnetic stir bar was charged the pthalic anhydride-d_4 (3.16 mmol), 1,2-dichlorobenzene (2 mL), and 3-(ethylamino)-*p*-cresol (2.95 mmol). A condenser was attached, and the solution was heated to 175 °C for 1 h. To the reaction was added 3-(ethylamino)-*p*-cresol (0.59 mmol) each hour for the next 5 h (2.95 mmol total). Following the final addition of 3-(ethylamino)-*p*-cresol , the reaction was stirred at 175 °C for an additional 12 h. The reaction mixture was cooled to ambient temperature, 3% aqueous sodium hydroxide (5 mL) was added with vigorous stirring, and the mixture was stirred for 30 min. The resulting rhodamine carboxylic acid solid was isolated by vacuum filtration. The unpurified carboxylic acid (537 mg) was dissolved in 3% H_2SO_4 in EtOH (10 mL) in a round-bottom flask containing a magnetic stir bar. A condenser was attached, and the solution was heated to 50 °C for 6 days. The reaction was cooled to ambient temperature and concentrated in vacuo. The unpurified residue was redissolved in ethanol (20 mL), and 14% aqueous solution of potassium bromide (10 mL) was added and the solution was stirred for 6 h. The resulting precipitated R6G-d_4 dye was isolated by vacuum filtration (380 mg, 0.720 mmol, 24% yield).

Ag Nanoparticle Synthesis. Following the procedure of Miesel et al., 90 mg of $AgNO_3$ was dissolved in 500 mL of water in a 1 L flask. After bringing the solution to a boil, 10 mL of a 1% sodium citrate solution was added while stirring rapidly. The solution was boiled for 30 min, during which the solution first turned transparent yellow and then finally opaque gray. After boiling, the nanoparticle solution was allowed to cool to room temperature and diluted to a final volume of approximately 420 mL. The majority of the nanoparticles prepared using

(9) Doering, W. E.; Nie, S. M. *J. Phys. Chem. B* **2002**, *106* (2), 311−317.
(10) LeRu, E. C.; Blackie, E.; Meyer, M.; Etchegoin, P. G. *J. Phys. Chem. C* **2007**, *111* (37), 13794−13803.
(11) Etchegoin, P. G.; Meyer, M.; Blackie, E.; LeRu, E. C. *Anal. Chem.* **2007**.
(12) Le Ru, E. C.; Meyer, M.; Etchegoin, P. G. *J. Phys. Chem. B* **2006**, *110* (4), 1944−1948.
(13) Goulet, P. J. G.; Aroca, R. F. *Anal. Chem.* **2007**, *79* (7), 2728−2734.
(14) Sawai, Y.; Takimoto, B.; Nabika, H.; Ajito, K.; Murakoshi, K. *J. Am. Chem. Soc.* **2007**, *129* (6), 1658−1662.
(15) Sharaabi, Y.; Shegai, T.; Haran, G. *Chem. Phys.* **2005**, *318* (1−2), 44−49.
(16) Haran, G. *Isr. J. Chem.* **2004**, *44* (4), 385−390.
(17) Jacobson, M. L.; Rowlen, K. L. *J. Phys. Chem. B* **2006**, *110* (39), 19491−19496.
(18) Zhang, D. M.; Xie, Y.; Deb, S. K.; Davison, V. J.; Ben-Amotz, D. *Anal. Chem.* **2005**, *77* (11), 3563−3569.
(19) Ramos, S. S.; Vilhena, A. F.; Santos, L.; Almeida, P. *Magn. Reson. Chem.* **2000**, *38* (6), 475−478.

this technique are spherical with an average diameter of 35 nm, but prisms, platelets, disks, and rods of various sizes are also present.

Instrumentation. The system was illuminated with $\lambda_{ex} = 532$ nm continuous wave laser light (Spectra Physics Millennia X) at grazing incidence. The approximate spot size after focusing was 1×2 mm^2 (excitation power density, $P_{ex} = 2.4$ W/cm^2), which is much larger than the field of view to aid in the locating of active spots. Inelastic Raman scattering was collected with an oil immersion objective equipped with a variable numerical aperture (NA) iris (Nikon 100X, NA 0.5) and a holographic notch filter (Kaiser) was placed in the microscope (Nikon TE300) to reject excitation light such that visual observation of the inelastic scattering was possible. The inelastic scattering was observable with the eye and appeared diffraction limited. The inelastic scattered light was analyzed with a 1/3 meter imaging spectrometer (Acton 300i) equipped with a LN_2-cooled CCD camera (Princeton Instruments Spec-10 400B). Individual diffraction-limited spots were centered on the spectrograph's entrance slit, and the Raman spectrum was collected. For measuring the localized surface plasmon resonance (LSPR) of the active SMSERS sites, the microscope was equipped with a dry dark field condenser (Nikon, NA = 0.7−0.95), and a low dispersion grating was inserted to collect the broadband spectrum. Electronic absorption experiments were performed on a UV/vis spectrometer (Ocean Optics S2000).

Sample Preparation I (SERS Characterization of Isotopologues). Silver island films (AgIF) were prepared by electron-beam deposition (Kurt J. Lesker Company, AXXIS system) of 6 nm of silver onto a glass slide. The AgIF were incubated in 10^{-6} M R6G-d_0 or R6G-d_4 in ethanol for 1 h, after which the sample was removed and rinsed with ethanol and dried with N_2. The instrumental setup was instead equipped with a 20× objective (Nikon) and the illumination was used in an epi configuration. (excitation power density, $P_{ex} = 15{,}000$ W/cm^2) The SER spectra of both isotopologues were collected from different AgIF samples.

Sample Preparation II (Environmental Control with Low Adsorbate Coverage). Chemically prepared Ag nanoparticles (ca. 10^{-9} M) were treated with R6G-d_0 (ca. 5×10^{-10} M) and R6G-d_4 (ca. 5×10^{-10} M) molecules such that approximately 0.5 R6G-d_0 and 0.5 R6G-d_4 were adsorbed per nanoparticle.[20] Statistically, there is nominally one molecule per nanoparticle, and it has equal probability of being R6G-d_0 or R6G-d_4, although the total number adsorbed will deviate according to the Poisson distribution. The nanoparticles were then treated with NaCl to cause aggregation, but at a low enough concentration (ca. 10 mM) such that precipitation of the nanoparticle aggregates did not occur.[21] A 10 μL aliquot of this solution was drop coated on a wet, base-treated (piranha etched and treated with a mixture of ammonia and hydrogen peroxide) No.1 glass coverslip (Fisher Scientific) to immobilize the nanoparticles. Samples were mounted in a custom-designed flow cell for environmental control and were exposed to dry N_2.

Sample Preparation III (High Adsorbate Coverage Under Ambient Conditions). Chemically prepared Ag nanoparticles (ca. 10^{-9} M) were treated with R6G-d_0 (ca. 5×10^{-8} M) and R6G-d_4 (ca. 5×10^{-8} M) molecules such that approximately 50 R6G-d_0 and 50 R6G-d_4 were adsorbed per nanoparticle.[20] Statistically, there are nominally 100 molecules per nanoparticle with a 1:1 ratio of R6G-d_0 or R6G-d_4, although the total number adsorbed will deviate according to the Poisson distribution. The nanoparticles were then treated with NaCl to cause aggregation, but at a low enough concentration (ca. 10 mM) such that precipitation of the nanoparticle aggregates did not occur.[21] A 10 μL aliquot of this solution was drop coated on a wet, base-treated No.1 glass coverslip (Fisher Scientific) to immobilize the nanoparticles. Samples were mounted on a custom-designed sample holder and left in ambient lab air.

(20) Lee, P. C.; Meisel, D. *J. Phys. Chem.* **1982**, *86* (17), 3391−3395.
(21) Meyer, M.; Le Ru, E. C.; Etchegoin, P. G. *J. Phys. Chem. B* **2006**, *110* (12), 6040−6047.

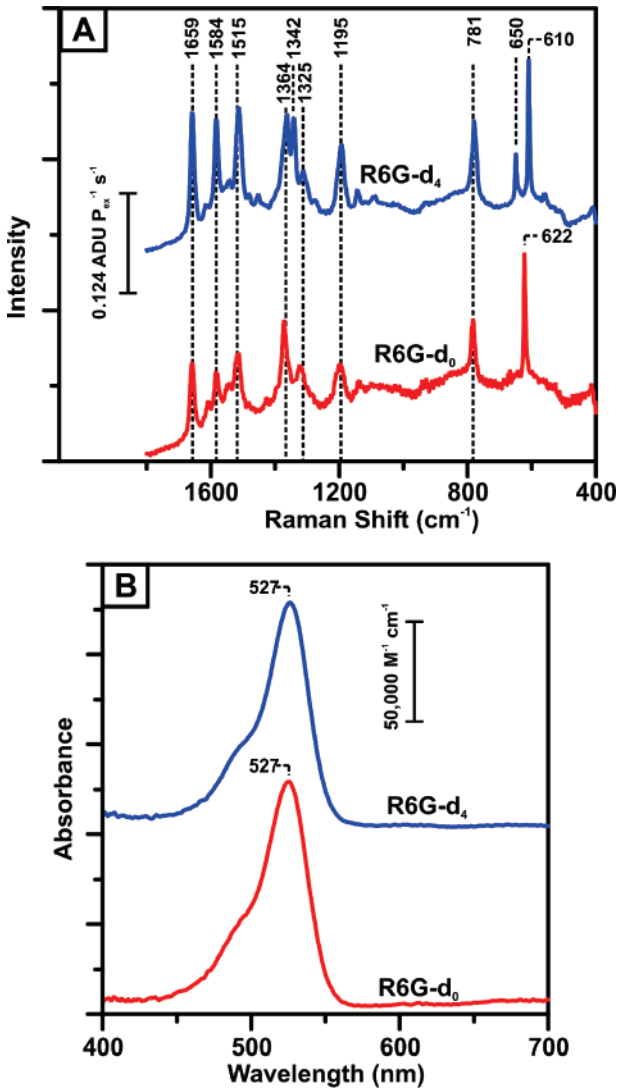

Figure 1. (A) SER spectra of the isotopologues adsorbed on separate Ag island film samples (6 nm Ag on glass coverslip) illustrating the differences in their vibrational character. ($\lambda_{ex} = 532$ nm, $t_{aq} = 150$ s, $P_{ex} = 15{,}000$ W/cm^2, epi illumination) (B) Visible absorption spectra of the isotopologues illustrating no perturbation of the electronic structure from isotopic substitution.

3. Results and Discussion

Figure 1A shows the ensemble-averaged SER spectrum of R6G-d_0 and R6G-d_4 adsorbed on separate 6 nm Ag island films. The major changes in the spectrum from the isotopic editing are a peak shift from 622 to 610 cm^{-1} and the presence of the 650 and 1342 cm^{-1} modes in R6G-d_4. There are small shifts in the remainder of the spectrum, but the presence of either the 622 or 610 cm^{-1} mode served as the discriminating factor in the analysis. The electronic absorption spectra of the two isotopologues are given in Figure 1B. The isotopic editing does not perturb the electronic structure of the molecule making isotopic editing an ideal procedure for bi-analyte SMSERS studies.

3.1. Environmental Control with Low Adsorbate Coverage. The SER spectra from 50 individual nanoparticle aggregates (identified as diffraction limited spots) were acquired across two different samples prepared using the same procedure. Only sites that were active were interrogated, and approximately 1 in 1000

sites observed though dark field scattering showed inelastic scattering observable to the eye. Figure 2A shows representative spectra from two of the spots measured, in which it is evident that there is only one isotopologue present in each probe volume. In a given spectrum, the analyte assignment was made by the sole presence of the 622 or 610 cm^{-1} mode, indicating that only R6G-d_0 or R6G-d_4 is present, respectively. If there was any indication that both peaks were present, it was counted as "both." A histogram of occurrences of all three possible cases is given in Figure 2B. Of the 50 spots sampled, 24 had solely R6G-d_4 character, 22 had solely R6G-d_0 character, and 4 showed character from both isotopologues. At the low coverage used (ca. 1 molecule per nanoparticle), the number of molecules adsorbed to the nanoparticles follows the Poisson distribution. Furthermore, the probability of measuring either isotopologue on the nanoparticle aggregate will be governed by the binomial distribution. The overall probability is given as the product of both distributions:

$$P(n_4,n_0,\alpha) = \frac{e^{-\alpha}\alpha^{n_4+n_0}}{(n_4+n_0)!} \times \frac{(n_4+n_0)!}{n_4!n_0!}\left(\frac{1}{2}\right)^{(n_4+n_0)} = \frac{e^{-\alpha}}{n_4!n_0!}\left(\frac{\alpha}{2}\right)^{(n_4+n_0)} \quad (1)$$

where n_4 and n_0 are the number of R6G-d_4 and R6G-d_0 molecules present in the SMSERS spectrum, respectively, and α is estimated number of molecules adsorbed per nanoparticle. This model does not take into account the fact that the entire nanoparticle surface does not have an EF adequate for SMSERS detection, and therefore, the probability of finding both in the hot spot should be lower than predicted. According to this model, 36.7% of the nanoparticles have no molecules present, 18.3% have a single R6G-d_4 molecule, 18.3% have a single R6G-d_0 molecule, 9.2% have one of each isotopologue 4.6% have two R6G-d_4, and 4.6% have two R6G-d_0. A table providing the probabilities for up to three of each isotopologue present is given in Table 1. Assuming that the four spectra that exhibit dual-analyte character originate from only two molecules (i.e., one R6G-d_0 and one R6G-d_4 on a single nanoparticle), then approximately two of the 24 R6G-d_4 only and two of the 22 R6G-d_0 only spectra should be due to multiple molecules of the same type. Based on eq 1, the R6G-d_4:both:R6G-d_0 probabilities should be 2.5:1:2.5; however, experimentally, the ratio is 6:1:5.5 as seen in Figure 2B. The suppression of the observation of both molecules is as predicted.

The 600−650 cm^{-1} portion of each spectrum was fit with a sum of Lorentzians. The principle 610 cm^{-1} peak coming from spectra denoted as R6G-d_4 actually varied from 605 to 612 cm^{-1}, while the principle 622 cm^{-1} peak from "R6G-d_0" spectra varied from 617 to 626 cm^{-1}. The degree of the spectral wandering observed is measured by a fit to the histograms seen in Figure 3A. The full width half-maximum (FWHM) of the R6G-d_4 Gaussian fit and R6G-d_0 Gaussian fit were 3.0 and 4.8 cm^{-1}, respectively. As a control, the normal Raman scattering of the 1028.3 cm^{-1} mode of cyclohexane was collected to illustrate the instrumentation stability. The FWHM of the Gaussian fit for this mode's spectral fluctuation was 0.6 cm^{-1}. The FWHM of the ensemble-averaged spectra were 5.3 cm^{-1} for R6G-d_4 and 6.9 cm^{-1} for R6G-d_0. The single-molecule results indicate that the ensemble-averaged spectrum is a superposition of the

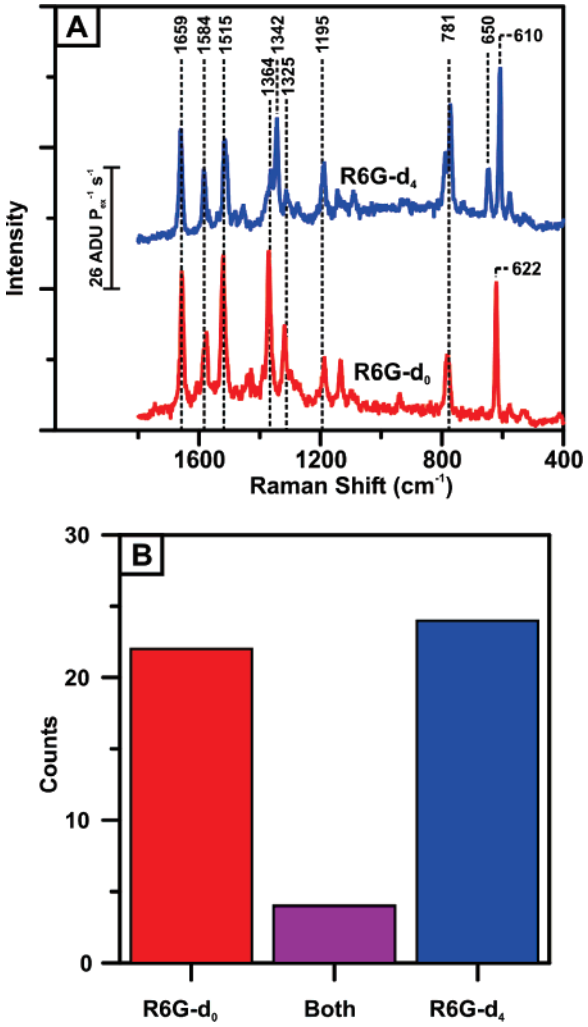

Figure 2. (A) Two representative spectra from the single-molecule results where one contains uniquely R6G-d_0 (red line) and the other uniquely R6G-d_4 (blue line) vibrational character. (λ_{ex} = 532 nm, t_{aq} = 10 s, P_{ex} = 2.4 W/cm^2, grazing incidence) (B) Histogram detailing the frequency with which only R6G-d_0, only R6G-d_4 and both R6G-d_0 and R6G-d_4 vibrational modes were observed with low adsorbate concentration under dry N_2 environment.

Table 1. Values from Eq 1 for Different Values of n_4 and n_0 Assuming a Concentration Parameter of $\alpha = 1$

n_4 n_0	0	1	2	3
0	36.79%	18.39%	4.60%	0.77%
1	18.39%	9.20%	2.30%	0.38%
2	4.60%	2.30%	0.57%	0.10%
3	0.77%	0.38%	0.10%	0.02%

single-molecule states. This analysis reveals the distribution of vibrational frequencies hidden under the ensemble average and shows that the ensemble population is heterogeneously broadened in a dry environment. Figure 3B confirms that the variation in intensity from one site to another is too large to observe quantized intensity from n = 1, 2, 3, etc. molecules as discussed by Pettinger et al.[8] and Etchegoin et al.[22,23]

The definitive proof for detection of fluorescence emission from a single molecule is photon anti-bunching, in which there is zero probability that two fluorescent photons will be emitted

(22) Etchegoin, P. G.; Meyer, M.; Le Ru, E. C. *Phys. Chem. Chem. Phys.* **2006**, *9*, 3006−3010.
(23) Le Ru, E. C.; Etchegoin, P. G.; Meyer, M. *J. Chem. Phys.* **2006**, *125* (20).

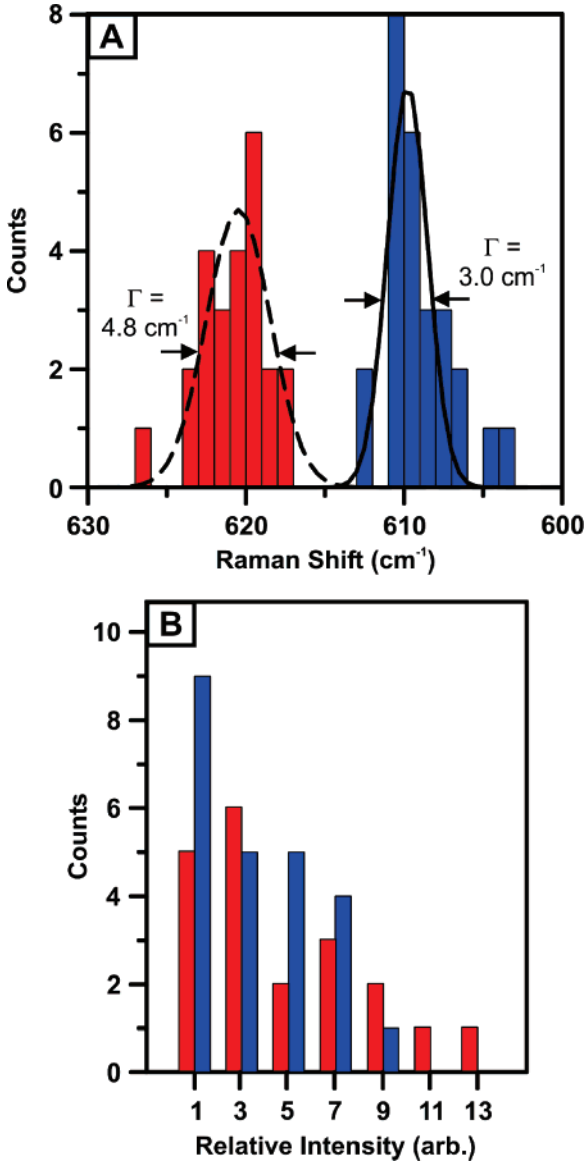

Figure 3. (A) Histogram of the low-frequency peak location for the events that exhibited single-molecule behavior, illustrating the degree of spectral changes observed for different sites. For R6G-d_0 (red data), the FWHM of the Gaussian fit was 4.8 cm^{-1}, and for R6G-d_4 (blue data), the FWHM of the Gaussian fit was 3.0 cm^{-1}. (B) Histogram of the characteristic peak intensity for the events that exhibited single-molecule behavior, illustrating the degree of intensity variations observed for different sites. R6G-d_0 (red data), R6G-d_4 (blue data).

at the same time due to the finite excited-state lifetime of the molecule.[24] Analogously, in this experiment, the spectra from the two different isotopologues are less likely to be observed than the individual component spectra if the spectrum is truly originating from a single molecule. While the system was under dry N_2, there was no evidence of time-dependent frequency fluctuations, and in most cases the spectral response appeared to be from a single source. Because a unique and stable frequency is observed for each vibrational mode in a given spectrum, the orientation and local environment of the molecule must not be changing; this is the origin of the relatively large frequency shifts from the ensemble-averaged value. (i.e., Figure 3A).

(24) Basche, T.; Moerner, W. E.; Orrit, M.; Talon, H. *Phys. Rev. Lett.* **1992**, *69* (10), 1516−1519.

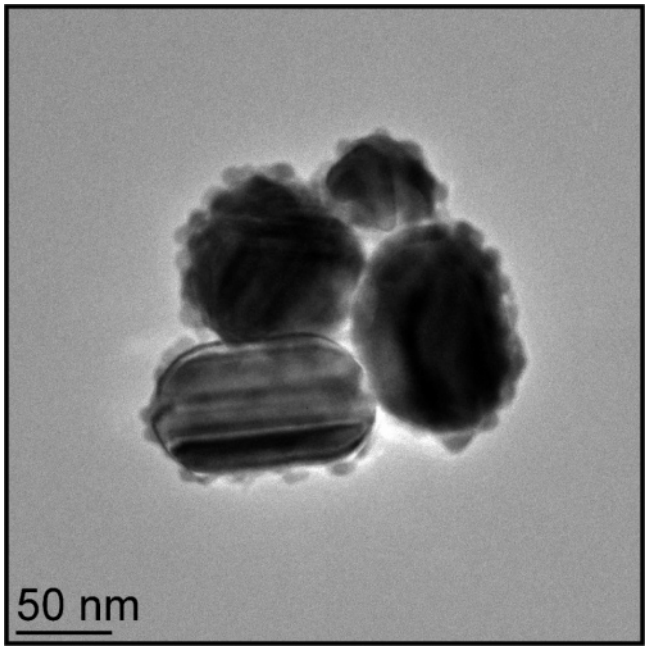

Figure 4. High-resolution transmission electron micrograph of an active SMSERS aggregate. Spectral data shown in Figure 5.

3.2. TEM, LSPR, and SMSERS Correlation. Under similar conditions, a TEM image of an active SMSERS aggregate is given in Figure 4, and the associated spectral data are given in Figure 5. Sample preparation remained the same as sample preparation II except that the 10 μL aliquot was placed on an indexed, polymer-coated transmission electron microscope (TEM) grid (Ted Pella PELCO Formvar). Both the Raman and LSPR images were collected for registration, and pattern matching allowed for correlation to the TEM image in a given grid square. Once the active junction was identified, the high-resolution image was collected. The SMSER spectrum in Figure 5A shows exclusively R6G-d_4 vibrational character. Also, the LSPR spectrum given in Figure 5B does not seem to have any relation to the excitation or Raman scattering frequencies. Ideally, for the maximum enhancement factor, the LSPR would be spectrally positioned in between these frequencies.[25] This result agrees with Brus et al.[5]

A general survey of active SMSERS aggregates revealed that they were composed of multiple nanoparticles, the included nanoparticles were not of any particular shape, and all aggregates contained nanoparticles of varying sizes. This might reveal some insight into the nature of SMSERS active sites as previous theoretical studies have focused on particles of the same size and shape at various orientations.[26] Additionally, the extinction of smaller particles is dominated by adsorption, whereas that of larger particles is dominated by scattering.[27] If small particles indeed play a role in active SMSERS junctions, then because the LSPR spectroscopy is performed by collecting scattering only, poor correlation is to be expected. Further theoretical studies need to be performed to investigate this further and are currently underway.

(25) McFarland, A. D.; Young, M. A.; Dieringer, J. A.; Van Duyne, R. P. *J. Phys. Chem. B* **2005**, *109* (22), 11279−11285.
(26) Hao, E.; Schatz, G. C. *J. Chem. Phys.* **2004**, *120* (1), 357−366.
(27) van Dijk, M. A.; Tchebotareva, A. L.; Orrit, M.; Lippitz, M.; Berciaud, S.; Lasne, D.; Cognet, L.; Lounis, B. *Phys. Chem. Chem. Phys.* **2006**, *8* (30), 3486−3495.

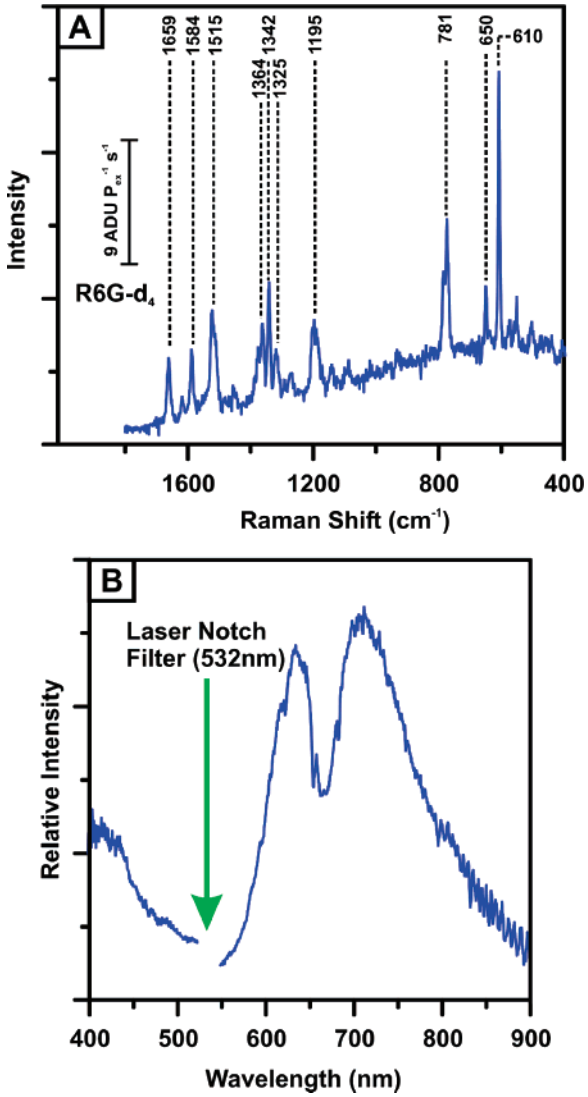

Figure 5. (A) SER spectrum exhibiting single-molecule behavior from the aggregate imaged in Figure 4. Spectrum shows uniquely R6G-d_4 vibrational character. ($\lambda_{ex} = 532$ nm, $t_{aq} = 10$ s, $P_{ex} = 8.0$ W/cm^2, grazing incidence, dry N_2) (B) Localized surface plasmon resonance scattering spectrum of the aggregate imaged in Figure 5. Disconnect at 532 nm corresponds to the notch filter centered at the SMSERS excitation wavelength.

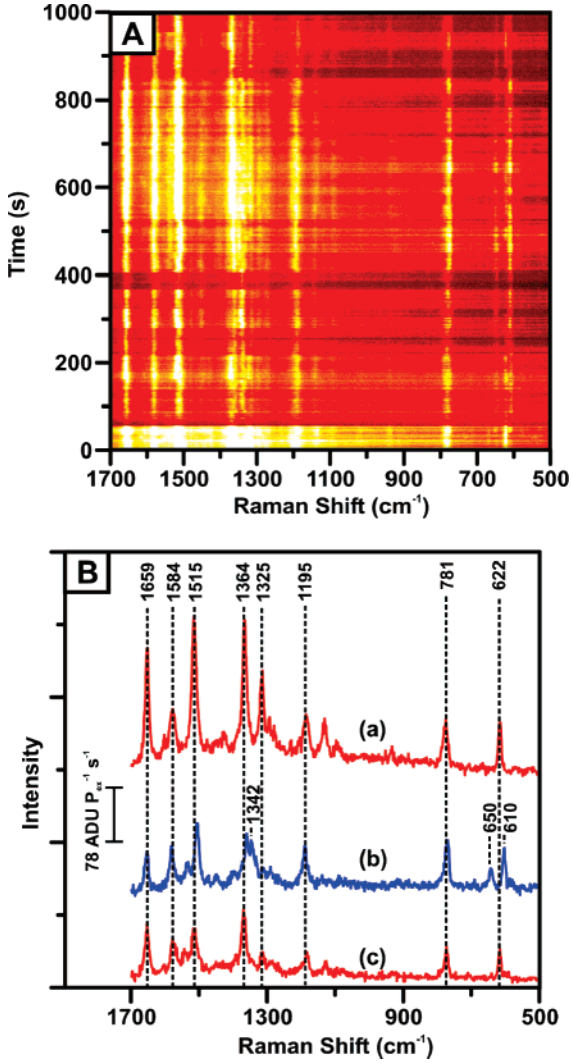

Figure 6. (A) Time series waterfall plot of spectra collected from a single active aggregate at high concentration in humid air. The false color represents signal intensity where white/yellow is highest and red/black is lowest. (B) Three time slices from the waterfall plot shown in (A) where (a) = 51 s, (b) = 463 s, and (c) = 936 s. The system changes state from R6G-d_0 to R6G-d_4 and back in 1000 s. ($\lambda_{ex} = 532$ nm, $t_{aq} = 1$ s, $P_{ex} = 2.4$ W/cm^2, grazing incidence).

3.3. High Adsorbate Coverage Under Ambient Conditions. When the system was under ambient environmental conditions (viz., humid air) at higher concentrations of molecules per nanoparticle, dynamic behavior, or "blinking", was observed. Statistically ca. 50 R6G-d_0 and 50 R6G-d_4 molecules were adsorbed per nanoparticle. Figure 6A shows a waterfall plot of inelastic scattering as a function of time. At $t = 0$ s, the spectrum appears to have only R6G-d_0 character, which is surprising considering the high dye concentration on the surface. The integrated intensity is on the same order of magnitude as the static, low concentration experiment above, indicating that only a single molecule is scattering and not the 100 in the ensemble. Therefore, the EF in the hot spot must be at least 3−4 orders of magnitude greater than the average SERS EF of the nanoparticle, in agreement with previously published results.[1,2] As time progresses, the spectrum changes completely from R6G-d_0 to R6G-d_4 and back to R6G-d_0 over the course of 1000 s as displayed in Figure 6B. The power of this experiment lies in the usage of two isotopologues that have identical surface binding chemistry.

The are two interpretations of the switching behavior considering that the SMSERS aggregates contain multiple potential hot spots: (1) two or more molecules are competing for the same hot spot on the nanoparticle surface, or (2) two or more molecules are acting independently at two different hot spots within a diffraction limited spot. Since these nanoparticles are highly aggregated, either is likely as it is possible for there to be multiple hot spots within a diffraction-limited spot. In an effort to distinguish which case is taking place, the data were analyzed with 2D cross correlation.[28] If there are independent hot spots in close proximity, then the time evolution of the 2 molecules should be noncorrelated ($\chi = 0$), but if it is the same hot spot, the molecules should be anti-correlated ($\chi = -1$). The

(28) Noda, I.; Ozaki, Y. *Two-Dimensional Correlation Spectroscopy: Applications in Vibrational and Optical Spectroscopy*; John Wiley and Sons, Ltd.: Chichester, West Sussex, 2004; p 295.

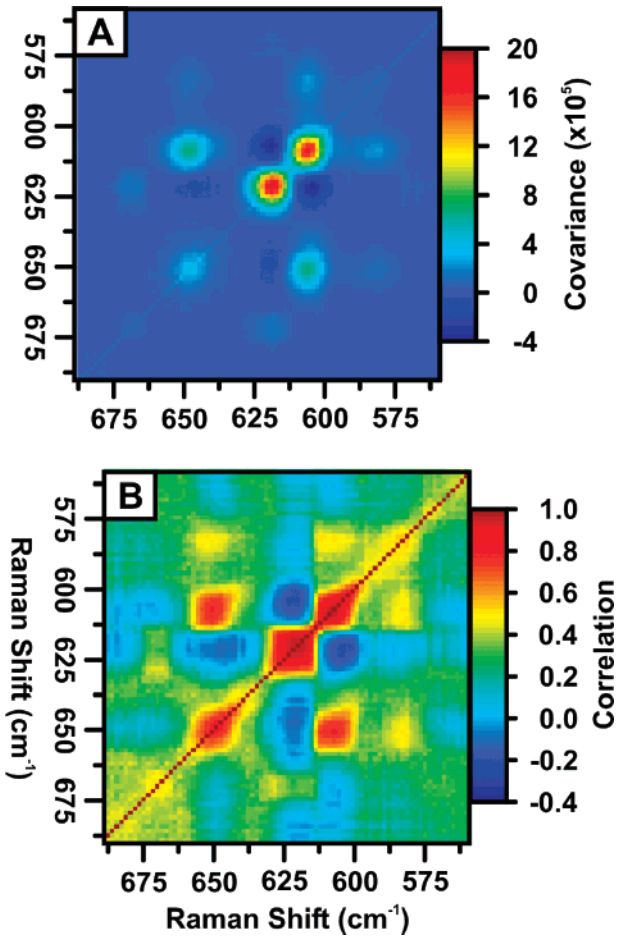

Figure 7. Zero time delay two-dimensional (A) covariance and (B) cross correlation of the time evolution data displayed in Figure 6.

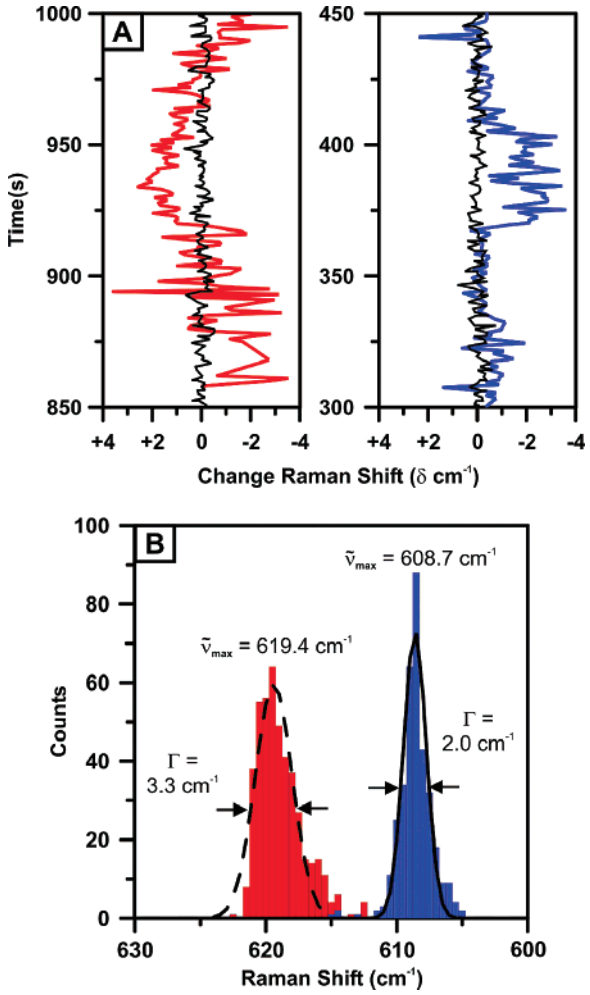

Figure 8. (A) Plot of the time evolution of spectral wandering present from the R6G-d_0 622 cm^{-1} mode (red data) and R6G-d_4 610 cm^{-1} mode (blue data) seen in Figure 3A. Only data points with intensity peaks that are greater than the limit of detection are shown. Black lines correspond to normal Raman scattering of the 1028.3 cm^{-1} mode of cyclohexane at comparable S/N as time evolution data with same acquisition time scale. The FWHM of the Gaussian fit for this mode's spectral fluctuation was 0.6 cm^{-1}. (B) Histogram displaying the bandwidth of the spectral wandering. For R6G-d_0 (red data), the FWHM of the Gaussian fit was 3.3 cm^{-1}, and for R6G-d_4 (blue data), the FWHM of the Gaussian fit was 2.0 cm^{-1}.

cross correlation between two Raman shifts, i and j, is given by:

$$\chi(i,j) = \frac{\sigma_{ij}}{\sqrt{\sigma_{ii}}\sqrt{\sigma_{jj}}} \tag{2}$$

where σ_{ij}, the covariance, is defined as:

$$\sigma_{ij} = \sum_{t=0} [\vec{I}(i,t) - \bar{I}(i)] \times [\vec{I}(j,t) - \bar{I}(j)] \tag{3}$$

and $I(n,t)$ is the intensity of the Raman shift n at time t and $I(x)$ is the time-averaged intensity of the given Raman shift, n. The cross correlation, $\chi(i,j)$, is calculated between all combinations of Raman shifts in the dataset. This method only concentrates on the zero time delay correlation, but it is possible to introduce a delay factor into the above equation to look for phase relationships in the dataset.

Figure 7A shows the covariance(σ_{ij}) and 7B shows the correlation ($\chi(i,j)$) in the region containing the characteristic bands of the isotopologues. They show strong correlation ($\chi = 0.8$) between 650 and 610 cm^{-1}, the two bands associated with R6G-d_4. Also, there is anti-correlation ($\chi = -0.3$) from bands associated with the cross-peaks between R6G-d_0 and R6G-d_4. In SERS, there is an intense, continuous background that covers the entire spectral region of interest. Rowland, Jonas et al. have shown that in this 2D cross-correlation analysis, there will be strong correlation of the Stokes bands to the continuum.[29] Therefore, even in the absence of a peak, there will be some time-correlated background contribution which will affect the peak-to-peak correlation. A linear trendline in the region of correlation was used to attempt to remove the background, but the correlation is sensitive to small changes in intensity and could not fully be removed. This is evident in the $\chi = 0.2-0.4$ correlation remaining between the background and the characteristic modes. This argues that the magnitude of the anti-correlation is larger, and therefore there is only one hot spot in the probe volume, and molecules are moving in short-range proximity to it. Unfortunately, it is impossible to determine if the signatures at $t = 51$ s and $t = 936$ s (both indicating R6G-d_0 character) are from the same molecule or two different R6G-d_0 molecules. Therefore, we are unable to discern if molecules are migrating into and out of the hot spot or if a molecule goes into a dark state while in the hot spot and if observed at a later

(29) Moore, A. A.; Jacobson, M. L.; Belabas, N.; Rowlen, K. L.; Jonas, D. M. *J. Am. Chem. Soc.* **2005**, *127* (20), 7292−7293.

time it is a new molecule, which is possible considering the relatively high coverage used in this experiment. In this high concentration regime, the dynamic behavior is caused not by a single molecule but due to the competition of a few molecules for access to the high EF hot spot.

In addition to this adsorbate switching behavior, spectral wandering was also observed in the dynamic experiment. Figure 8A shows the Raman shift versus time for two modes, the 610 cm^{-1} mode of R6G-d_4 and the 622 cm^{-1} mode of R6G-d_0. A histogram of vibrational frequencies (Figure 8B) shows the same trend as the static measurement, but the FWHM of the Gaussian fit is narrower. For R6G-d_0, the FWHM of the Gaussian fit was 3.3 cm^{-1}, and for R6G-d_4, the FWHM of the Gaussian fit was 2.0 cm^{-1}. In the dynamic system, there is no environmental control which allows a hydration layer to form on the nanoparticle surface. This layer allows for diffusion of the isotopologues into and out of the hot spot, but also allows the isotopologue to sample many configurations during the acquisition time. Therefore, the distribution of observed frequency trajectories in the dynamic system is narrower than the static case as this hydration layer is not present in the static system.

4.Conclusions

The data presented here support four main conclusions. First, this work offers a strong proof for the existence of single-molecule SERS based on frequency, rather than intensity, correlation. The static, low coverage case shows that, when approximately one molecule per nanoparticle was adsorbed, only one type of molecule is present in the SER spectrum. The probability of observing only one isotopologue follows a combined Poissonian-binomial distribution. Second, the spectral width of the ensemble-averaged spectrum correlates with the distribution of frequencies at the single-molecule level. These variations are most likely due to differences in interactions between the surface and individual molecules; therefore, the ensemble-averaged system is probing the superposition of all surface states. Third, SMSERS active aggregates are composed of multiple randomly sized and shaped nanoparticles. Fourth, the isotope editing also provides insight into the nature of the dynamic behavior present in SMSERS under certain conditions. Specifically, at the high concentration and ambient conditions present in this report, the dynamic behavior was not from a single molecule but from a few molecules diffusing into and out of a single hot spot as revealed by cross correlation. Consequently, the size of the hot spot must be on the same order as that of R6G itself. Spectral wandering is also observed in this case, but to a smaller degree due to the hydration layer present from the humid conditions.

Acknowledgment. We gratefully acknowledge Dr. Leif Sherry, Dr. Yingmin Wang, and Prof. Laurence Marks for the TEM experiments. We also thank Dr. Katherine A. Willets for many helpful discussions about single-molecule spectroscopy. This work was supported by the National Science Foundation (CHE-0414554, DMR-0520513, EEC-0647560, BES-0507036), the Air Force Office of Scientific Research (MURI Grant F49620-02-1-0381), and the DTRA JSTO Program (Grant FA9550-06-1-0558).

JA077243C